Bioorganic Chemistry 86 (2019) 686–695

Contents lists available at ScienceDirect

Bioorganic Chemistry

journal homepage: www.elsevier.com/locate/bioorg

Synthesis and characterization of CAPE derivatives as xanthine oxidase inhibitors with radical scavenging properties

Wonbeen Choi[a], Valente Villegas[a], Hannah Istre[b], Ben Heppler[b], Niki Gonzalez[b], Nicole Brusman[b], Lindsey Snider[b], Emily Hogle[b], Janelle Tucker[b], Alma Oñate[b], Sandra Oñate[b], Lili Ma[b], Stefan Paula[a,c,*]

[a] Department of Chemistry, Purdue University, 560 Oval Drive, West Lafayette, IN 47907-2084, USA
[b] Department of Chemistry and Biochemistry, Northern Kentucky University, Nunn Drive, Highland Heights, KY 41099-1905, USA
[c] Department of Biochemistry, Purdue University, 175 South University Street, West Lafayette, IN 47907-2063, USA

ARTICLE INFO

Keywords:
Caffeic acid derivatives
Radical scavenging
Enzyme inhibition
Dual properties
Ligand docking
Knoevenagel condensation

ABSTRACT

Inhibitors of the enzyme xanthine oxidase (XO) with radical scavenging properties hold promise as novel agents against reperfusion injuries after ischemic events. By suppressing the formation of damaging reactive oxygen species (ROS) by XO or scavenging ROS from other sources, these compounds may prevent a buildup of ROS in the aftermath of a heart attack or stroke. To combine these two properties in a single molecule, we synthesized and characterized the non-purine XO inhibitor caffeic acid phenethylester (CAPE) and 19 derivatives using a convenient microwave-assisted Knoevenagel condensation protocol. Varying systematically the number and positions of the hydroxyl groups at the two phenyl rings, we derived structure-activity relationships based on experimentally determined XO inhibition data. Molecular docking suggested that critical enzyme/inhibitor interactions involved π-π interactions between the phenolic inhibitor ring and Tyr914, hydrogen bonds between inhibitor hydroxyl groups and Glu802, and hydrophobic interactions between the CAPE phenyl ring and nonpolar residues located at the entrance of the binding site. To effectively scavenge the stable radical DPPH, two hydroxyl groups in 1,2- or 1,4-position at the phenyl ring were required. Among all compounds tested, *E*-phenyl 3-(3,4-dihydroxyphenyl)acrylate, a CAPE analog without the ethyl tether, showed the most promising properties.

1. Introduction

The natural product caffeic acid phenethyl ester (CAPE) is found in a variety of plants and is also a component of honey bee propolis [1]. It is a hydrophobic polyphenol composed of a catechol (ring A) and a phenyl ring (ring B) which are connected by a tether containing an ester group and an (*E*)-carbon-carbon double bond (Fig. 1). CAPE has a number of interesting bioactivities, some of which have therapeutic potential. In 1988, the seminal article by Grunberger and coworkers described for the first time CAPE's isolation from propolis, its chemical characterization, and its synthesis [2]. However, even long before this study, CAPE had been used in a variety of folk remedies against a number of ailments, thereby alluding to its therapeutic potential. Subsequent studies described some of CAPE's antimicrobial properties, its anti-inflammatory effects, and its toxicity to cancer cells [3–5]. Many of these properties have been attributed to CAPE's antioxidant qualities, enabling it to absorb reactive oxygen species (ROS) that could otherwise damage tissue. Other properties of CAPE, however, are the result of it acting as a specific enzyme inhibitor in the traditional sense by binding to a specific pocket in a target protein and shutting down its activity [6].

A well-known bioactivity of CAPE is its ability to inhibit the activity of the enzyme xanthine oxidase (XO) with a potency in the low micromolar range [7,8]. Kinetic studies identified it as a competitive inhibitor, implying that it binds at the same site as the natural substrates xanthine and hypoxanthine [9]. For decades, XO inhibition has been the mainstay therapeutic strategy for the treatment of hyperuricemia, which manifests itself in elevated blood levels of uric acid [10,11]. These in turn can cause kidney disease, cardiovascular problems, and gout. The latter condition frequently results in inflammatory arthritis as uric acid crystals accumulate in joints. By suppressing the formation of uric acid through the inhibition of XO, this build-up of crystals can be prevented as the more soluble precursors or uric acid xanthine and hypoxanthine are excreted through the kidneys [10–12]. At the present

* Corresponding author at: Department of Chemistry, Purdue University, 560 Oval Drive, West Lafayette, IN 47907-2084, USA.
E-mail address: paulas@purdue.edu (S. Paula).

https://doi.org/10.1016/j.bioorg.2019.02.049
Received 20 December 2018; Received in revised form 24 January 2019; Accepted 21 February 2019
Available online 22 February 2019
0045-2068/

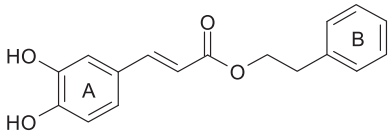

Fig. 1. The chemical structure of CAPE.

time, there are two drugs in clinical use that inhibit XO. Allopurinol, a purine-based compound, is a prototype XO inhibitor and has been used for decades. Febuxostat, an XO inhibitor with a different, non-purine scaffold, has entered the market more recently and features an increased potency in comparison to allopurinol, whose high dosage levels are known to make side effects such as renal failure or Stephens-Johnson syndrome more likely [12]. In addition, other non-purine inhibitors scaffolds that might avoid allopurinol's side effects have been explored in non-clinical settings. These include pyrazolines [13], β-acetamido compounds [14], azaflavones [15], naphthopyrans [16], and pyrimidinones [17]. Alternative treatments of hyperuricemia that are presently explored comprise interleukin-1 inhibitors, effectors of renal urate transporters, and the use of recombinant uricase [18–20]. Nevertheless, XO inhibition continues to be the first-line therapy for hyperuricemia, which is why the development of new XO inhibitors remains a rather active field of pharmacological research today.

In addition to the treatment of hyperuricemia, XO inhibition has been proposed as a potential remedy for reperfusion injuries which can occur in the aftermath of ischemic events such as heart attacks or strokes [21–23]. During these events, oxygen supply to the affected tissue is temporarily blocked, which causes XO activity to cease since oxygen is one of the enzyme's substrates. As a result, the other two XO substrates – xanthine and hypoxanthine – start to accumulate, which is why XO resumes its activity at markedly increased rates once blood circulation and the concomitant oxygen supply have been reestablished. Since XO produces the highly reactive oxygen species (ROS) hydrogen peroxide and/or the superoxide ion as byproducts, the suppression of excessive XO activity by inhibitors is thought to prevent tissue damage by elevated ROS levels [24,25].

As we have demonstrated recently for coumarin and chalcone derivatives, the protective effect of XO inhibitors in cells subjected to oxidatively generated stress is enhanced if these compounds also possess radical scavenging activities, enabling them to absorb ROS generated by sources other than XO [26,27]. Unfortunately, the structural optimization of the chalcone and particularly of the coumarin scaffolds were limited because their small sizes offered few opportunities for chemical modifications. Therefore, we turned to the somewhat larger CAPE scaffold as a suitable alternative for further exploration. In addition to these considerations, we considered CAPE as an attractive target because of its reported ability to suppress reperfusion injuries in rats [28–30] and its use, in the form of propolis, to treat skin burns, which can be regarded as a form of reperfusion injury as they cause ischemia in the affected tissue.

Historically, CAPE was first synthesized at Columbia University in 1988 through acid-catalyzed (*p*-toluene sulfonic acid) esterification of caffeic acid with phenethyl alcohol in benzene [2]. Other methods to synthesize CAPE analogs were developed in subsequent years. For example, CAPE derivatives were prepared from caffeic acid and phenethyl alcohol through an acyl transfer reaction [31], from caffeic acid and β-phenyl bromide by a S_N2 dicyclohexylcarbodiimide coupling reaction [32], or from 3,4-dihydroxybenzaldehyde and phosphonate ester by the Wittig reaction [33]. Despite its simple structure, the synthesis of CAPE or CAPE derivatives by these methods is limited due to requirements for corrosive catalysts, toxic solvents, protecting groups, and long reaction times and they frequently suffer from low yields. Additionally, these methods limit the installation of various functional groups on the CAPE scaffold. In 2005, Xia and coworkers reported the synthesis of CAPE analogs from malonic acid, phenethyl alcohol, and 3,4-dihydroxybenzaldehyde by malonic acid monoester formation followed by Knoevenagel condensation [34]. This method was further improved by replacing malonic acid with Meldrum's acid [35].

Here, we present a rapid and efficient microwave-assisted synthetic route to CAPE and a pool of 19 derivatives with diverse structural features based on Knoevenagel condensation. The compounds varied with regard to the number and position of hydroxyl groups present at the phenyl rings, length of the tether, and chemical composition of the hydrophobic residue equivalent to the phenethyl group in CAPE (Figs. 2 and 3). The compounds' XO inhibitory potencies and radical scavenging abilities were evaluated in assays whose results were the basis for structure-activity relationships (SARs) that linked the molecular structure of these compounds to their activities. Molecular docking provided insight into the interactions critical for inhibitor binding. Overall, our analysis delineated the structural requirements necessary for good inhibitory potency and for radical scavenging ability, with the ultimate goal of establishing the basis for the design of novel agents capable of protecting tissue from oxidative damage.

2. Experimental section

2.1. Chemistry

Reagents and solvents, including compounds **2**, **3**, **4**, and **7**, were obtained from Aldrich or Fisher Scientific and used without further purification unless otherwise noted. Microwave-assisted reactions were conducted with a MultiwavePro microwave reaction system from Anton Paar Instruments (Vernon Hills, IL). The pressure vessels consisted of disposable Wheaton® glass vials (Item# 224882) with a special PEEK screw cap and a PTFE seal (Reaction volume 0.3 – 3 mL, operation pressure: 20 bar). A rotor (4 × 24MG5) and four SiC well-plates were used for homogeneous heating of up to 96 g-scale experiments in parallel. Thin-layer chromatography was performed using precoated silica gel F254 plates (Whatman). Bromocresol green stain solution was used as the visualization agent for malonic acid monoesters and a $KMnO_4$ solution was used as visualization agent for CAPE derivatives. Column chromatography was performed with pre-packed RediSep Rf Silica columns on a CombiFlash Rf Flash Chromatography system (Teledyne Isco). NMR spectra were obtained on a Joel 500 MHz spectrometer. Chemical shifts were reported in parts per million (ppm) relative to the tetramethylsilane signal at 0.00 ppm. Coupling constants (*J*) were reported in Hertz (Hz). The peak patterns were indicated as follows: s, singlet; d, doublet; t, triplet; dt, doublet of triplet; dd, doublet of doublet; m, multiplet; q, quartet. Mass spectra were obtained on a Waters TQD Tandem Quadrupole Mass Spectrometer and data were collected in the electrospray positive mode. High resolution mass spectra were recorded on a Micromass Q-TOF 2 or a Thermo Scientific LTQ-FT™ mass spectrometer operating in electrospray mode.

2.2. General procedure - Method A, thermal conditions

Malonic acid monoester formation. A mixture of Meldrum's acid (4.8 mmol, 1.2 equiv., 0.69 g) and the corresponding alcohol (4 mmol, 1.0 equiv.) in dioxane (10 mL) was heated under reflux conditions overnight (95–110 °C for 18 – 24 h). After the removal of the dioxane solvent by rotatory evaporation, the residue was separated using a column of Diaion HP-20, eluting with H_2O, 30% CH_3OH/H_2O and CH_3OH to give the desired malonic acid monoesters as a light yellow oil.

Caffeic acid phenyl ester derivatives. The desired amount of malonic acid monoesters (0.6 mmol, 1.2 equiv.) was dissolved in toluene (1 mL) followed by the addition of pyridine (12.5 mmol, 25 equiv., 1 mL) and piperidine (0.80 mmol, 1.6 equiv., 79 μL). This mixture was stirred at r.t. for 10 min to form enolates before the desired aldehyde (0.5 mmol, 1.0 equiv.) was added at 0 °C. The reaction mixture was continued to be stirred at r.t. for 1 ~ 6 days. TLC was used to monitor the reaction progress. Once the reaction was complete, the reaction mixture was transferred to a separatory funnel using EtOAc (15 mL) and washed

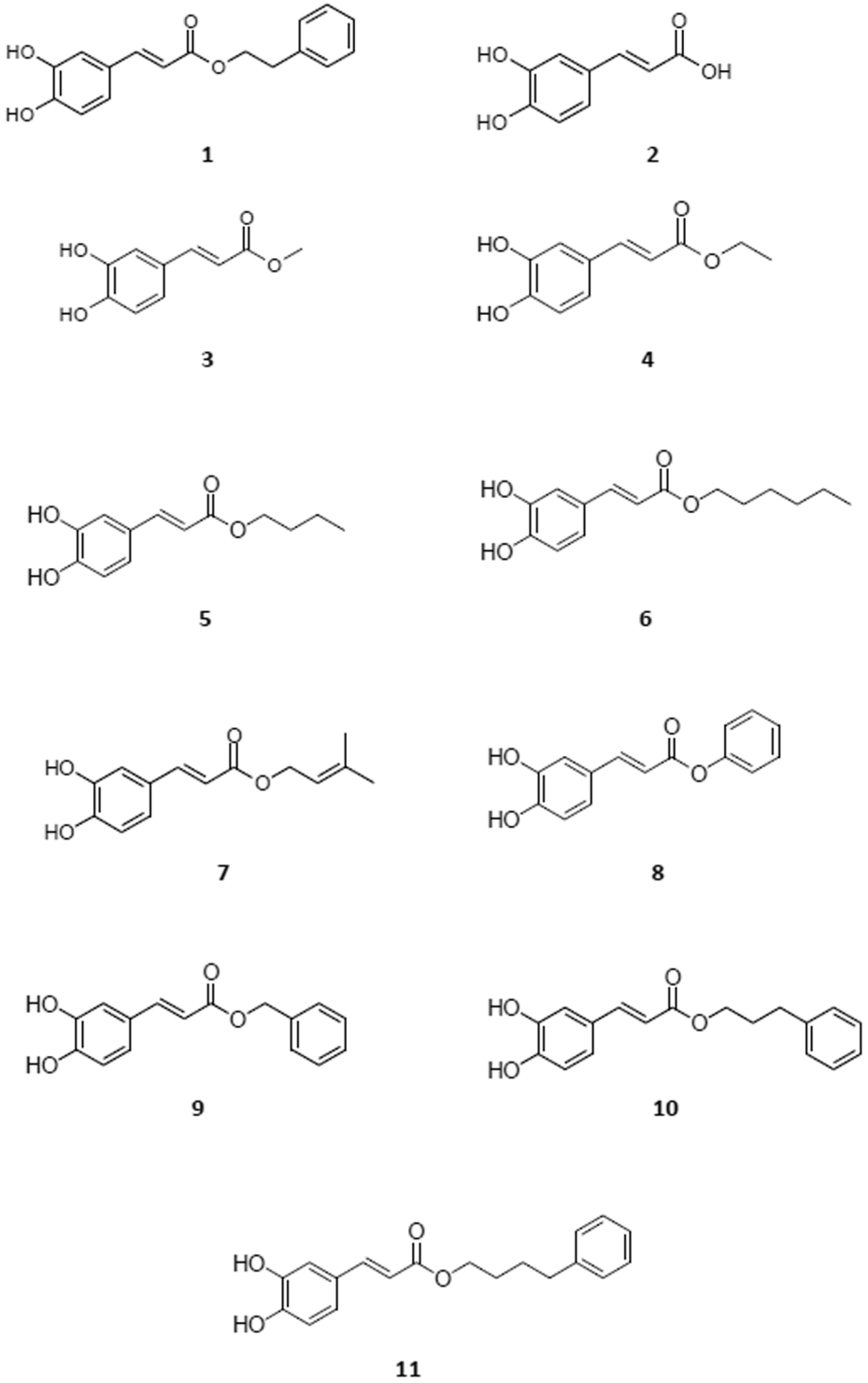

Fig. 2. CAPE analogs with modifications about the B-ring and tether moiety.

with 5% HCl (10 mL × 2) and distilled water (10 mL × 2). After removal of the ethyl acetate by rotatory evaporation, the crude product was purified by automated flash chromatography, eluting with an ethyl acetate/hexanes or methanol/methylene chloride gradient to afford the desired products.

2.3. General procedure - Method B, microwave irradiation

Malonic acid monoester formation. A mixture of Meldrum's acid (4.8 mmol, 1.2 equiv., 0.69 g) and the corresponding alcohol (4 mmol, 1.0 equiv.) in dioxane (3 mL) was heated by microwave irradiation at 140 °C for 5 min. After the removal of the dioxane by rotatory evaporation, the residue was separated using a column of Diaion HP-20, eluting with H_2O, 30% CH_3OH/H_2O and CH_3OH to give the desired malonic acid monoesters as a light yellow oil.

Caffeic acid phenyl ester derivatives. The desired amount of malonic acid monoesters (0.6 mmol, 1.2 equiv.) was dissolved in toluene (1 mL) followed by the addition of pyridine (12.5 mmol, 25 equiv., 1 mL) and piperidine (0.80 mmol, 1.6 equiv., 79 μL). This mixture was stirred at r.t. for 10 min to form enolates before the desired aldehyde (0.5 mmol, 1.0

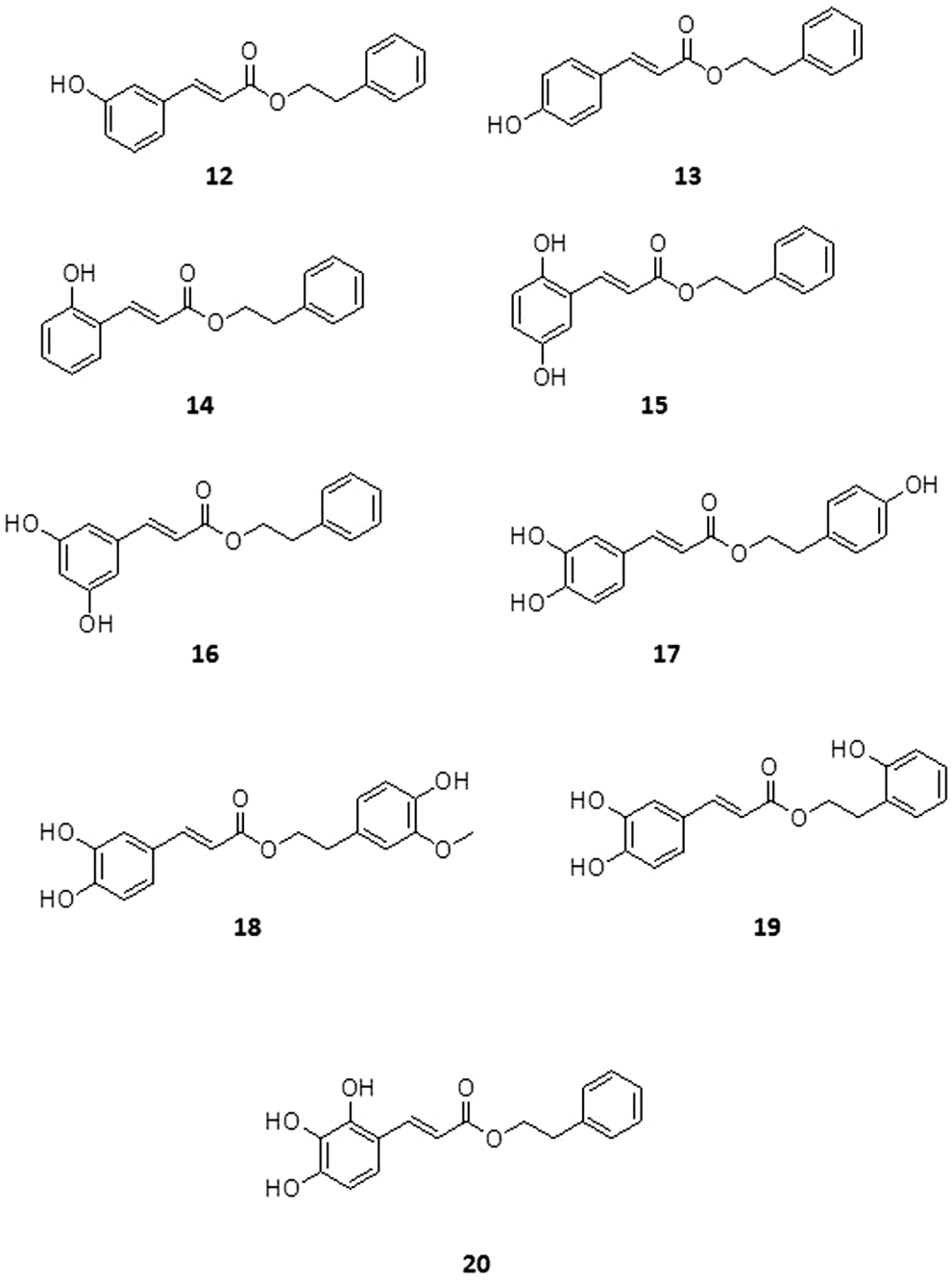

Fig. 3. CAPE analogs with modifications of the hydroxyl substitution pattern.

equiv.) was added at 0 °C. The reaction mixture was continued to be stirred at 0 °C for one hour, followed by microwave irradiation at 120 °C for 10 min. TLC was used to monitor the reaction progress. Once the reaction was complete, the reaction mixture was transferred to a separatory funnel using EtOAc (15 mL) and washed with 5% HCl (10 mL × 2) and distilled water (10 mL × 2). After the removal of the ethyl acetate by rotatory evaporation, the crude product was purified by automated flash chromatography, eluting with an ethyl acetate/hexanes or methanol/methylene chloride gradient to afford the desired products.

2.4. (E)-phenethyl 3-(3,4-dihydroxyphenyl)acrylate (1)

Synthesized from Meldrum's acid, 2-phenylethanol and 3,4-dihydroxybenzaldehyde according to the general procedure Method A (thermal conditions) described above. White solid. Yield: 68.2%. ^{1}H NMR ($CDCl_3$, 500 MHz, ppm): δ 7.56 (1H, d, J = 16.1 Hz), 7.31–7.25 (5H, m), 7.08 (1H, d, J = 2.3 Hz), 7.02 (1H, d, J = 7.8 Hz), 6.87 (1H, d, J = 8.2 Hz), 6.22 (1H, d, J = 15.6 Hz), 4.41 (2H, t, J = 7.4 Hz), 3.01 (2H, t, J = 6.9 Hz). ^{13}C NMR ($CDCl_3$, 125 MHz, ppm): δ 167.8, 146.5, 145.3, 143.9, 137.9, 129.0, 128.6, 127.5, 126.7, 122.6, 115.6, 115.4, 114.5, 65.3, 35.3. HRMS: Calculated for $C_{17}H_{15}O_4$ [M − H] 283.0970, found 283.0973.

2.5. (E)-butyl 3-(3,4-dihydroxyphenyl)acrylate (5)

Synthesized from Meldrum's acid, 1-butanol and 3,4-dihydroxybenzaldehyde according to the general procedure Method A (thermal conditions) described above. Light yellow oil. Yield: 75.8%. ^{1}H NMR ($CDCl_3$, 500 MHz, ppm): δ 7.53 (1H, d, J = 15.6 Hz), 7.07 (1H, d, J = 1.8 Hz), 6.91 (1H, d, J = 8.3 Hz), 6.84 (1H, d, J = 7.8 Hz), 6.21

(1H, d, J = 16.0 Hz), 4.16 (2H, t, J = 6.4 Hz), 1.67–1.62 (2H, m), 1.43–1.36 (2H, m), 0.92 (3H, t, J = 7.3 Hz). ^{13}C NMR ($CDCl_3$, 125 MHz, ppm): δ 168.2, 147.2, 145.3, 144.7, 127.1, 122.2, 115.6, 115.1, 114.4, 64.6, 30.8, 19.3, 13.8. HRMS: Calculated for $C_{13}H_{15}O_4$ [M−H] 235.0970, found 235.0969.

2.6. (E)-hexyl 3-(3,4-dihydroxyphenyl)acrylate (6)

Synthesized from Meldrum's acid, hexan-1-ol and 3,4-dihydroxybenzaldehyde according to the general procedure Method A (thermal conditions) described above. White solid. Yield: 74.3%. ^{1}H NMR ($CDCl_3$, 500 MHz, ppm): δ 7.57 (1H, d, J = 16.0 Hz), 7.09 (1H, d, J = 1.9 Hz), 7.00 (1H, dd, J = 2.3 Hz, 8.3 Hz), 6.87 (1H, d, J = 16.0 Hz), 6.26 (1H, d, J = 16.0 Hz), 4.18 (2H, t, J = 6.5 Hz), 1.71–1.64 (4H, m), 1.40–1.26 (4H, m), 0.89 (3H, t, J = 2.3 Hz). ^{13}C NMR ($CDCl_3$, 125 MHz, ppm): δ 167.9, 147.2, 145.1, 144.8, 126.9, 121.9, 115.5, 115.2, 114.3, 64.6, 31.5, 28.8, 25.7, 22.6, 14.1; HRMS: Calculated for $C_{15}H_{19}O_4$ [M−H] 263.1283, found 263.1282.

2.7. (E)-phenyl 3-(3,4-dihydroxyphenyl)acrylate (8)

Synthesized from Meldrum's acid, phenol and 3,4-dihydroxybenzaldehyde according to the general procedure Method A (thermal conditions) described above. White solid. Yield: 53.0%. ^{1}H NMR (acetone-d_6, 500 MHz, ppm): δ 8.57 (1H, br s), 8.27 (1H, br s), 7.72 (1H, d, J = 16.0 Hz), 7.42 (2H, t, J = 8.0 Hz), 7.25 (1H, t, J = 7.8 Hz), 7.24 (1H, s), 7.18 (2H, d, J = 8.2 Hz), 7.14 (1H, dd, J = 2.3, 2.3 Hz), 6.90 (1H,d, J = 8.2 Hz), 6.50 (1H, d, J = 15.5). ^{13}C NMR (acetone-d_6, 125 MHz, ppm): δ 179.5, 165.2, 151.4, 148.4, 146.8, 145.5, 129.3, 125.5, 122.2, 121.9, 115.7, 114.7, 113.8. HRMS: Calculated for $C_{15}H_{11}O_4$ [M−H] 255.0657, found 255.0655.

2.8. (E)-benzyl 3-(3,4-dihydroxyphenyl)acrylate (9)

Synthesized from Meldrum's acid, benzyl alcohol and 3,4-dihydroxybenzaldehyde according to the general procedure Method A (thermal conditions) described above. White solid. Yield: 82.9%. ^{1}H NMR (acetone-d_6, 500 MHz, ppm): δ 8.52 (1H, br s), 8.24 (1H, br s), 7.58 (1H, d, J = 16.1 Hz), 7.44–7.32 (5H, m), 7.16 (1H, s), 7.05 (1H, d, J = 8.2 Hz), 6.86 (1H, d, J = 8.2 Hz), 6.34 (1H, d, J = 15.6 Hz), 5.21 (2H, s). ^{13}C NMR (acetone-d_6, 125 MHz, ppm): δ 166.5, 148.1, 145.5, 145.3, 137.0, 128.5, 128.1, 128.0, 126.8, 121.8, 115.6, 114.6, 114.5, 65.5. HRMS: Calculated for $C_{16}H_{13}O_4$ [M−H] 269.0814, found 269.0817.

2.9. (E)-3-phenylpropyl 3-(3,4-dihydroxyphenyl)acrylate (10)

Synthesized from Meldrum's acid, 3-phenylpropan-1-ol and 3,4-dihydroxybenzaldehyde according to the general procedure Method A (thermal conditions) described above. White solid. Yield: 69.3%. ^{1}H NMR ($CDCl_3$, 500 MHz, ppm): δ 7.57 (1H, d, J = 15.6 Hz), 7.29–7.25 (2H, m), 7.21–7.18 (3H, m), 7.11 (1H, d, J = 1.9 Hz), 7.02 (1H, d, J = 8.0 Hz), 6.88 (1H, d, J = 8.4 Hz), 6.27 (1H, d, J = 16.0 Hz), 4.22 (2H, t, J = 6.9 Hz), 2.74 (2H, t, J = 7.8 Hz), 2.06–2.02 (2H, m). ^{13}C NMR ($CDCl_3$, 125 MHz, ppm): δ 167.8, 146.5, 145.2, 143.6, 140.8, 128.6, 128.5, 127.6, 126.1, 122.2, 115.6, 115.5, 114.5, 64.2, 32.3, 30.4. HRMS: Calculated for $C_{18}H_{17}O_4$ [M−H] 297.1286, found 297.1285.

2.10. (E)-4-phenylbutyl 3-(3,4-dihydroxyphenyl)acrylate (11)

Synthesized from Meldrum's acid, 4-phenyl-1-butanol and 3,4-dihydroxybenzaldehyde according to the general procedure Method A (thermal conditions) described above. White solid. Yield: 65.2%. ^{1}H NMR ($CDCl_3$, 500 MHz, ppm): δ 7.57 (1H, d, J = 16.1 Hz), 7.30–7.15 (5H, m), 7.10 (1H, s), 6.98 (1H, dd, J = 1.5 Hz, 8.3 Hz), 6.87 (1H, d, J = 8.3 Hz), 6.25 (1H, d, J = 16.1 Hz), 4.21 (2H, m), 2.65 (2H, m), 1.75–1.67 (4H, m). ^{13}C NMR ($CDCl_3$, 125 MHz, ppm): δ 168.4, 146.7, 145.4, 144.0, 142.1, 128.5, 128.5, 127.4, 126.0, 122.5, 115.6, 115.4, 114.5, 64.8, 35.5, 28.4, 27.8. HRMS: Calculated for $C_{19}H_{19}O_4$ [M−H] 311.1283, found 311.1288.

2.11. (E)-phenethyl 3-(3-hydroxyphenyl)acrylate (12)

Synthesized from Meldrum's acid, 2-phenylethanol and 3-hydroxybenzaldehyde according to the general procedure Method A (thermal conditions) described above. White solid. Yield: 79.4%. ^{1}H NMR ($CDCl_3$, 500 MHz, ppm): δ 7.60 (1H, d, J = 15.6 Hz), 7.33–7.23 (8H, m), 6.98 (1H, s), 6.38 (1H, d, J = 16.0 Hz), 4.41 (2H, t, J = 7.4 Hz), 3.01 (2H, t, J = 6.9 Hz). ^{13}C NMR (CDCl3, 125 MHz, ppm): δ 167.5, 145.2, 137.8, 135.8, 130.5, 130.2, 129.0, 128.7, 126.7, 120.8, 118.2, 117.8, 114.7, 65.5, 35.2. HRMS: Calculated for $C_{17}H_{15}O_3$ [M−H] 267.1021, found 267.1021.

2.12. (E)-phenethyl 3-(4-hydroxyphenyl)acrylate (13)

Synthesized from Meldrum's acid, 2-phenylethanol and 4-hydroxybenzaldehyde according to the general procedure Method A (thermal conditions) described above. White solid. Yield: 82.8%. ^{1}H NMR ($CDCl_3$, 500 MHz, ppm): δ 7.62 (1H, d, J = 15.6 Hz), δ 7.41 (2H, d, J = 6.9 Hz), 7.26–7.23 (5H, m), 6.85 (2H, d, J = 6.8 Hz), 6.63 (1H, br s), 6.28 (1H, d, J = 16.1 Hz), 4.41 (2H, t, J = 6.9 Hz), 3.01 (2H, t, J = 6.9 Hz). ^{13}C NMR ($CDCl_3$, 125 MHz, ppm): δ 167.8, 157.8, 145.0, 137.6, 132.6, 130.1, 129.9, 129.0, 128.6, 126.7, 116.1, 65.2, 35.3. HRMS: Calculated for $C_{17}H_{15}O_3$ [M−H] 267.1021, found 267.1018.

2.13. (E)-phenethyl 3-(2-hydroxyphenyl)acrylate (14)

Synthesized from Meldrum's acid, 2-phenylethanol and 2-hydroxybenzaldehyde according to the general procedure Method B (microwave irradiation) described above. White solid. Yield: 34.3%. ^{1}H NMR ($CDCl_3$, 500 MHz, ppm): δ 8.01 (1H, d, J = 16.0 Hz), 7.45 (1H, d, J = 7.4 Hz), 7.33–7.22 (7H, m), 6.83 (1H, d, J = 7.8 Hz), 6.60 (1H, d, J = 16.5 Hz), 4.43 (2H, t, J = 7.4 Hz), 3.02 (2H, t, J = 7.3 Hz). ^{13}C NMR ($CDCl_3$, 125 MHz, ppm): δ 167.8, 154.9, 140.7, 137.9, 134.5, 131.5, 129.0, 128.6, 126.6, 121.7, 120.8, 118.4, 116.5, 65.2, 35.3. HRMS: Calculated for $C_{17}H_{15}O_3$ [M−H] 267.1021, found 267.1021.

2.14. (E)-phenethyl 3-(2,5-dihydroxyphenyl)acrylate (15)

Synthesized from Meldrum's acid, 2-phenylethanol and 2,5-dihydroxybenzaldehyde according to the general procedure Method B (microwave irradiation) described above. White solid. Yield: 30.2%. ^{1}H NMR (acetone-d_6, 500 MHz, ppm): δ 8.78 (2H, br s), 7.60 (1H, d, J = 16.1 Hz), 7.41 (1H, d, J = 2.1 Hz), 7.37–7.16 (5H, m), 7.12 (1H, d, J = 7.8 Hz), 6.92 (1H, d, J = 7.3 Hz), 6.45 (1H, d, J = 16.1 Hz), 4.37 (2H, t, J = 6.9 Hz), 2.99 (2H, t, J = 6.8 Hz). ^{13}C NMR (acetone-d_6, 125 MHz, ppm): δ 166.3, 158.1, 144.7, 138.4, 130.4, 130.1, 129.0, 128.5, 126.5, 121.7, 119.8, 118.1, 114.8, 64.8, 35.0. HRMS: Calculated for $C_{17}H_{17}O_4$ [M+H] 285.1127, found 285.1125.

2.15. (E)-phenethyl 3-(3,5-dihydroxyphenyl)acrylate (16)

Synthesized from Meldrum's acid, 2-phenylethanol and 3,5-dihydroxybenzaldehyde according to the general procedure Method B (microwave irradiation) described above. White solid. Yield: 66.2%. ^{1}H NMR (acetone-d_6, 500 MHz, ppm): δ 8.61 (2H, br S), 7.50 (1H, d, J = 16.0 Hz), 7.31–7.19 (5H, m), 6.89 (1H, d, J = 2.2 Hz), 6.62 (2H, d, J = 2.3 Hz), 6.37 (1H, d, J = 16.1 Hz), 4.36 (2H, t, J = 7.8 Hz), 2.98 (2H, t, J = 7.8 Hz). ^{13}C NMR ($CDCl_3$, 125 MHz, ppm): δ 192.0, 166.2, 159.0, 145.0, 136.4, 128.5, 126.5, 117.9, 107.7, 106.7, 105.0, 64.8, 35.0. HRMS: Calculated for $C_{17}H_{15}O_4$ [M−H] 283.0970, found

283.0968.

2.16. (E)-4-hydroxyphenethyl 3-(3,4-dihydroxyphenyl)acrylate (17)

Synthesized from Meldrum's acid, 2-(4-hydroxyphenyl)ethanol and 3,4-dihydroxybenzaldehyde according to the general procedure Method B (microwave irradiation) described above. White solid. Yield: 64.8%. ^{1}H NMR (acetone-d_6, 500 MHz, ppm): δ 8.42 (2H, br s), 8.21 (1H, br s), 7.52 (1H, d, J = 16.1 Hz), 7.14 (1H, d, J = 1.9 Hz), 7.11 (2H, d, J = 8.3 Hz), 7.02 (1H, d, J = 7.9 Hz), 6.85 (1H, d, J = 8.3 Hz), 6.77 (2H, d, J = 6.4 Hz), 6.26 (1H, d, J = 16.0 Hz), 4.27 (2H, t, J = 6.9 Hz), 2.89 (2H, t, J = 7.3 Hz). ^{13}C NMR (acetone-d_6, 125 MHz, ppm): δ 166.7, 156.1, 148.0, 145.5, 144.9, 130.0, 129.0, 126.8, 121.8, 115.6, 115.3, 114.8, 114.4, 64.9, 34.2. HRMS: Calculated for $C_{17}H_{17}O_5$ [M + H] 301.1076, found 301.1076.

2.17. (E)-4-hydroxy-3-methoxyphenethyl 3-(3,4-dihydroxyphenyl) acrylate (18)

Synthesized from Meldrum's acid, homovanillyl alcohol and 3,4-dihydroxybenzaldehyde according to the general procedure Method B (microwave irradiation) described above. White solid. Yield: 75.5%. ^{1}H NMR (acetone-d_6, 500 MHz, ppm): δ 8.33 (1H, br s), 7.53 (1H, d, J = 16.0 Hz), 7.14 (1H, d, J = 1.8 Hz), 7.03 (1H, dd, J = 8.2 Hz, 1.9 Hz), 6.90 (1H, s), 6.86 (1H, d, J = 8.2 Hz), 6.76–6.72 (2H, m), 6.27 (1H, d, J = 16.1 Hz), 4.29 (2H, t, J = 7.3 Hz), 3.82 (3H, s), 2.89 (2H, t, J = 6.9 Hz). ^{13}C NMR (acetone-d_6, 125 MHz, ppm): δ 179.1, 166.3, 147.8, 147.4, 145.6, 145.3, 144.9, 129.6, 126.9, 121.7, 121.5, 115.6, 114.9, 114.4, 112.5, 64.9, 55.4, 34.7. HRMS: Calculated for $C_{18}H_{17}O_6$ [M − H] 329.1025, found 329.1025.

2.18. (E)-2-hydroxyphenethyl 3-(3,4-dihydroxyphenyl)acrylate (19)

Synthesized from Meldrum's acid, 2-hydroxyphenethyl alcohol and 3,4-dihydroxybenzaldehyde according to the general procedure Method B (microwave irradiation) described above. White solid. Yield: 49.2%. ^{1}H NMR (acetone-d_6, 500 MHz, ppm): δ 8.38 (1H, br s), 7.52 (1H, d, J = 16.0 Hz), 7.17 (1H, dd, J = 7.8 Hz, 1.9 Hz), 7.14 (1H, d, J = 1.9 Hz), 7.07–6.99 (2H, m), 6.86–6.84 (2H, m), 6.78 (1H, td, J = 7.3 Hz, 0.9 Hz), 6.26 (1H, d, J = 16.0 Hz), 4.34 (2H, t, J = 7.4 Hz), 2.99 (2H, t, J = 7.4 Hz). ^{13}C NMR (acetone-d_6, 125 MHz, ppm): δ 179.8, 166.6, 155.4, 151.5, 147.9, 145.5, 144.8, 130.9, 127.7, 121.7, 119.6, 115.6, 115.0, 114.4, 106.7, 63.3, 29.8; HRMS: Calculated for $C_{17}H_{15}O_5$ [M − H] 299.0919, found 299.0921.

2.19. (E)-phenethyl 3-(2,3,4-trihydroxyphenyl)acrylate (20)

Synthesized from Meldrum's acid, 2-phenylethanol and 2,3,4-trihydroxybenzaldehyde according to the general procedure Method B (microwave irradiation) described above. White solid. Yield: 34.6%. ^{1}H NMR (acetone-d_6, 500 MHz, ppm): δ 7.89 (1H, d, J = 16.1 Hz), 7.31–7.23 (5H, m), 7.04 (1H, d, J = 8.2 Hz), 6.98 (1H, d, J = 8.3 Hz), 6.47 (1H, d, J = 16.0 Hz), 6.44 (1H, d, J = 7.6 Hz), 4.34 (2H, t, J = 6.6 Hz), 2.99 (2H, t, J = 6.9 Hz). ^{13}C NMR (acetone-d_6, 125 MHz, ppm): δ 167.1, 147.8, 146.7, 140.8, 138.5, 132.6, 129.0, 128.4, 126.4, 120.3, 114.8, 112.3, 111.9, 64.3, 35.1. HRMS: Calculated for $C_{17}H_{15}O_5$ [M − H] 299.0919, found 299.0914.

2.20. Determination of inhibitory potency against XO activity

Bovine XO, xanthine, and potassium phosphate were received from Sigma. The rate of XO-catalyzed conversion of xanthine to uric acid was determined spectroscopically with a Cary 300 UV/Vis spectrophotometer by measuring the concomitant absorbance increase at 295 nm for several minutes [10]. XO (0.14 units/mg) was suspended in buffer (25 mM phosphate, pH 7.5) and the reaction was initiated by adding the enzyme buffer (final XO concentration: 39 μg/mL) to xanthine dissolved in the same buffer (final concentration: 50 μM; total volume: 200 μL), using micro plastic cuvettes capable of transmitting UV light. Assays were conducted in the absence and presence of test compounds at 11 different concentrations. Reaction rates were obtained by linear regression of the absorbance versus time traces and then fit to a three-parameter logistic equation. Inhibitory potencies were expressed as IC_{50} values, the inhibitor concentration that reduced XO activity by 50% [36]. To make the comparison of potencies convenient, IC_{50} values were converted into relative inhibitory potencies (RIP) by dividing the IC_{50} value of a given compound by that of the reference compound CAPE (IC_{50}: 3.9 μM).

2.21. Measurement of DPPH scavenging activities

The radical 2,2-diphenyl-1-picrylhydrazyl (DPPH) and ethanol were obtained from Sigma. The radical scavenging abilities of compounds were assessed using the stable radical DPPH as a model species, which is a commonly employed approach [37]. Assays were conducted by mixing 50 μL of a freshly prepared solution of DPPH in ethanol (0.2 mM) with 150 μL of the test compound in ethanol to give a final concentration of 20 μM. Samples were placed in a 96-well plate and incubated for 30 min at room temperature in the dark. The decrease in DPPH absorbance at a wavelength of 517 nm, an indicator of radical scavenging, was measured with a plate reader (Epoch 2, Biotek, Winooski). Radical scavenging activity (RSA) was then calculated from the DPPH absorbance as follows:

$$\text{activity} = (1 - A_{test}/A_{control})\,100\%$$

As a positive control, assays were performed with the known antioxidant ascorbic acid.

2.22. Molecular modelling of inhibitor binding to XO

The structures of all ligands to be analyzed were modelled with the modelling suite MOE (Molecular Open Environment, Chemical Computing Group, Montreal, Canada) [38] and their conformations were energy-minimized using Molecular Mechanics in combination with the MMFF94x force field. The crystal structure of XO in complex with xanthine was obtained from the Protein Databank (PDB code: 3EUB [39]). All entries other than the protein, cofactors, and xanthine were deleted. The protein structure was protonated and the positions of the added protons were optimized via Molecular Mechanics with the Amber10 force field. Since CAPE is a competitive inhibitor of XO [9], the binding site into which the compounds were docked was defined by the position of the xanthine molecule in the crystal structure. Subsequent docking was performed with MOE's default settings, using the triangle matcher method in conjunction with the London dG scoring function for the initial placement of the ligand [40]. The rigid receptor setting with the GBVI/WSA scoring function was employed for the refinement of the 30 top poses. Analysis and visualization of the docking output, including the identification of hydrogen bonds, steric clashes, hydrophobic interactions, or π–π interactions were performed in MOE. In a control run, the previously deleted xanthine molecule was docked back into the XO binding site and the observed agreement between the obtained pose and the pose seen in the crystal structure validated the accuracy of the docking protocol.

3. Results and discussion

3.1. Synthesis of CAPE derivatives

The synthesis of CAPE and its derivatives is summarized in Scheme 1. Briefly, Meldrum's acid and the corresponding alcohol in dioxane were heated under microwave irradiation at 140 °C for 5 min to form the malonic acid monoester. Catalyzed by piperidine, the purified

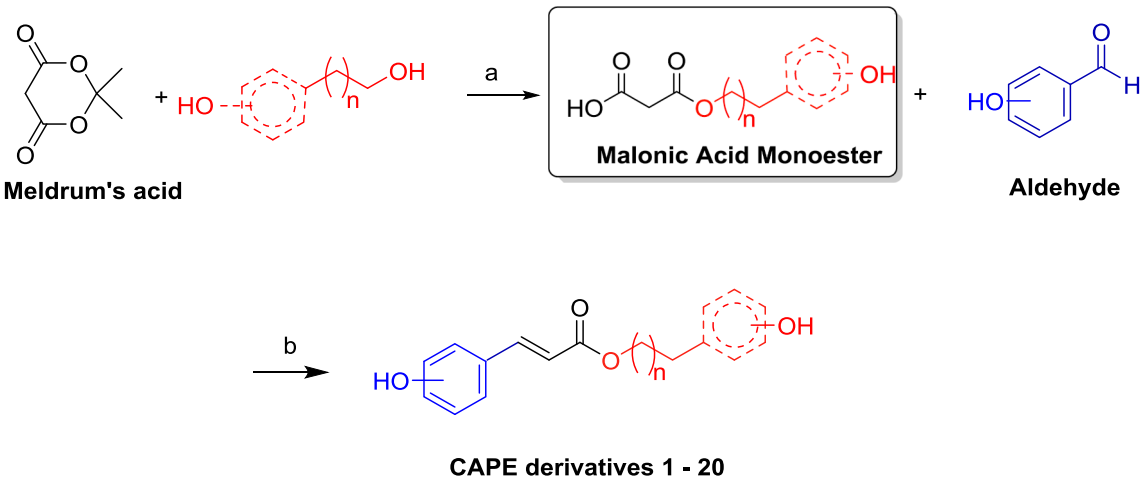

Scheme 1. Synthesis of CAPE derivatives under thermal and microwave conditions. Conventional heating: (a) Dioxane, 1 eq alcohol, 1.2 eq Meldrum's acid, reflux conditions overnight (95–110 °C); (b) 1 eq aldehyde, 1.2 eq monoester, 1.6 eq piperidine, 25 eq pyridine, rt, 1–6 days. Microwave irradiation: (a) Dioxane, 1 eq alcohol, 1.2 eq Meldrum's acid, MW 140 °C, 5 min; (b) 1 eq aldehyde, 1.2 eq monoester, 1.6 eq piperidine, 25 eq pyridine, MW, 120 °C, 10 min.

malonic acid monoester was then allowed to react with the desired aldehyde in toluene/pyridine under microwave irradiation at 120 °C for 10 min. Compared with traditional thermal heating, the reaction time was reduced from overnight (18–24 h) to 5 min for the first step and from 1 to 6 days to 10 min for the second step, which constitutes a drastic improvement. Additionally, the amount of solvent was reduced significantly when using the microwave approach.

Simple CAPE derivatives (compounds **1**–**13**) could be synthesized by either using thermal heating or microwave irradiation. Other CAPE analogs (e.g. compounds **14**–**20**) were more challenging to obtain by traditional thermal heating. Those compounds tended to have more than two hydroxyl groups or a hydroxyl group located in *ortho* position with respect to the carbon–carbon double bond. Microwave irradiation proved to be a successful method to prepare these compounds with reasonable yields. All synthesized compounds were fully characterized by ^{1}H NMR and ^{13}C NMR spectroscopy and by HRMS. ^{1}H NMR spectra revealed that the olefinic bond was in the *E* configuration, an observation that was further supported by coupling constants of the two olefinic protons around 16 Hz.

3.2. Structure-activity relationships of XO inhibition

As shown in Table 1, all compounds tested displayed measurable potencies, covering a relatively narrow window of RIP values of about two orders of magnitude between 0.069 (**8**, best) and 8.4 (**12**, worst).

Table 1
XO activity inhibition and DPPH radical scavenging activities of compounds. Inhibitory activity is expressed as relative inhibitory potency (RIP), obtained by dividing the IC_{50} value (see "Materials and Methods") of a given compounds by that of CAPE. The experimental error of the assay was determined to be ± 20%. Radical scavenging abilities (RSA) were calculated as described in "Materials and Methods" and quantified as percentages.

Compound	*RIP*	*RSA*	*Compound*	*RIP*	*RSA*
1	1.0	57	**11**	4.8	69
2	1.3	72	**12**	8.4	−7
3	0.79	72	**13**	3.3	−2
4	1.1	72	**14**	2.0	−2
5	3.2	63	**15**	4.1	67
6	1.7	67	**16**	1.5	−5
7	0.31	74	**17**	0.29	59
8	0.069	67	**18**	0.84	60
9	0.18	62	**19**	0.18	70
10	1.9	58	**20**	1.3	66

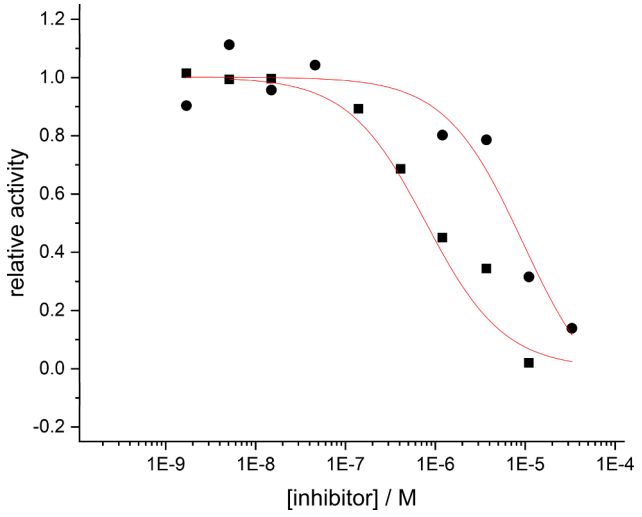

Fig. 4. Representative XO activity inhibition assay for the most active (**8**, squares) and one of the less active (**13**, circles) compounds. Lines were obtained by non-linear fitting of the data to a three-parameter logistic equation.

Fig. 4 shows the results of two representative inhibition assays (**8** and **13**). The RIP of **8** was based on an IC_{50} value of about 250 nM, suggesting that it is a less potent inhibitor than febuxostat whose potency has been reported by others [41] or measured by us in the low nanomolar or subnanomolar range. However, it compares rather favorably with the potency of allopurinol that we obtained under similar conditions (IC_{50}: 3.5 µM).

The results indicated that the complete removal of the phenethyl moiety (**2**) or its replacement by a significantly smaller methyl (**3**) or ethyl group (**4**) had little effect on potency. Interestingly, the introduction of the two longer, unbranched alkyl chains (**5**: butyl; **6**: hexyl) was detrimental to potency. Shortening of the ethyl tether attached to the B-ring resulted in the highest activities observed in the compound pool (**8** and **9**) whereas its lengthening caused a slight loss in potency (**10** and **11**). The branched and monounsaturated chain of **7** conveyed good potency.

Removal of one of the two hydroxyl groups at the A-ring of **1** reduced potency (**12** and **13**), whereas the removal of one of the two hydroxyl groups in **15** resulted in the opposite (**14**). Comparing the activities of **15** and **16** to that of **1** showed that the 3,4-substitution pattern seen in CAPE was superior to a 3,5- or a 2,5-pattern. The

introduction of a third hydroxyl group in 1-position at the A-ring (**20**) had no effect on potency. However, if a third hydroxyl group was placed on the B-ring at the opposite side of the molecule, increased potencies were noticed (**17**, **18**, and **19**).

3.3. Structural basis for inhibitor binding to XO

In order to provide a depiction of the ligand/receptor interactions and rationalize the observed SARs for XO inhibition at the molecular level, we docked the structure of CAPE into the enzyme's X-ray crystal structure (Fig. 5). This computational approach was necessitated by the unavailability of crystal structures of XO in complex with CAPE or CAPE derivatives. The interaction diagram (Fig. 5C) showed that most of the critical ligand/receptor interactions occurred around the A-Ring of CAPE. Glu802 formed a hydrogen bond with one of the hydroxyl groups and π–π stacking interactions were observed between Phe914 and the A-ring (Fig. 5B). The hydrogen bond explained the need for hydroxyl groups of CAPE for binding, but it did not account for the finer nuances seen for variations in the hydroxyl substitution pattern. However, it should be noted that hydroxyl groups could have interacted with the binding site in ways other than just by hydrogen bonding. Steric clashes and unfavorable contacts with hydrophobic residues in the back of the binding site as observed for some of the compounds were such possibilities. Moreover, shape complementarity seemed to be of general importance as the apparent tight fit between ligand and receptor suggested the presence of substantial van-der-Waals interactions and hydroxyl groups may have served in that capacity as well. (see Fig. 6)

The binding pocket had a predominantly hydrophobic character that accommodated the non-polar parts of the inhibitors, such as the two phenyl rings and parts of the connecting tether. Interestingly, the entrance of the binding site had an amphiphilic character (Fig. 5D), with one side being mainly hydrophobic (Leu648, Phe1013, and Leu1014) and the opposite side predominately hydrophilic (Ser876 and Lys771). As a result, the B ring of CAPE which was sandwiched between these two areas did not ideally match the hydrophobicity/

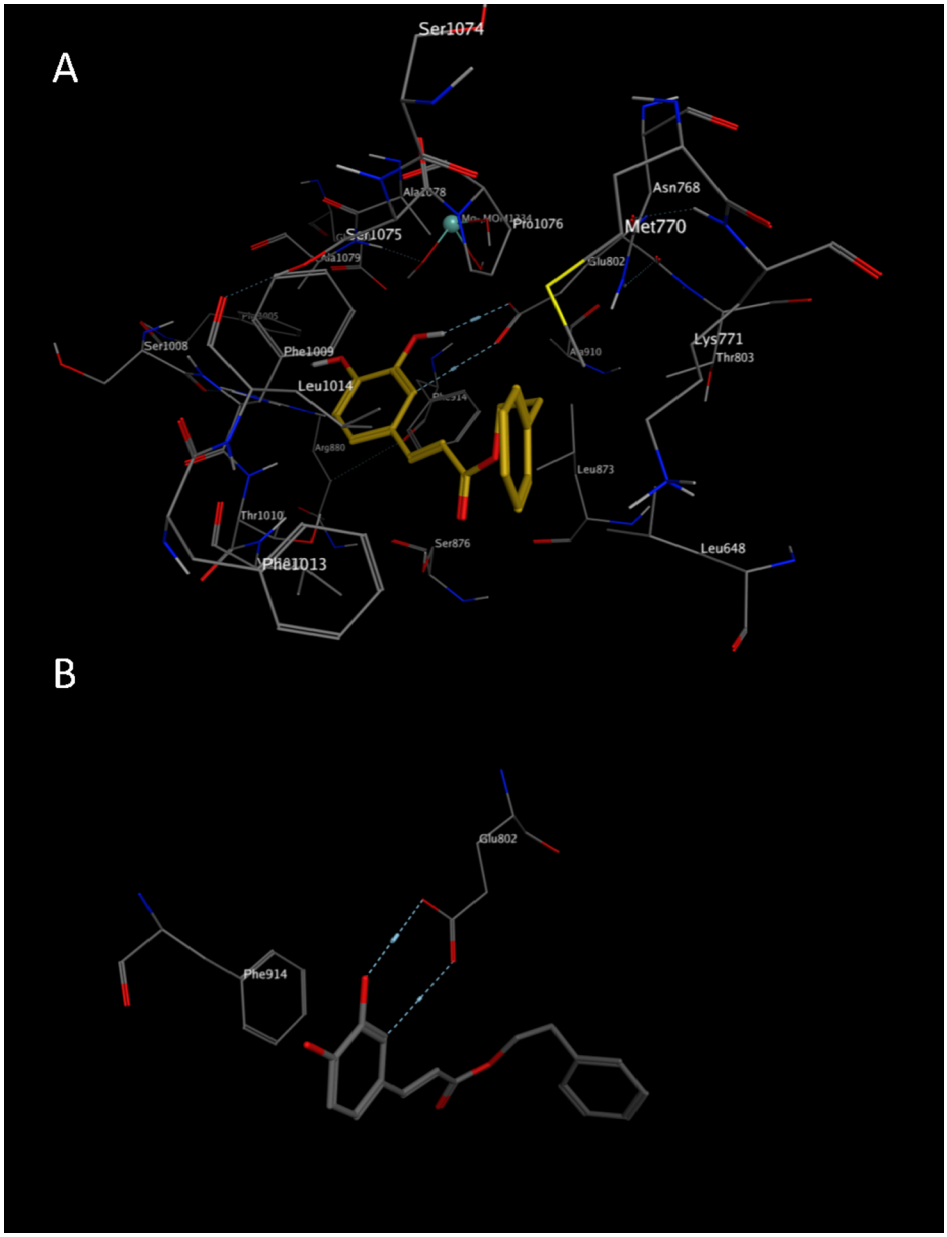

Fig. 5. CAPE docked into the binding site of XO. A: Complete binding site. CAPE is shown in yellow. B: 3D representation of two critical residues engaging in hydrogen bonds (Glu 802) and π–π interactions (Phe 914) with CAPE.

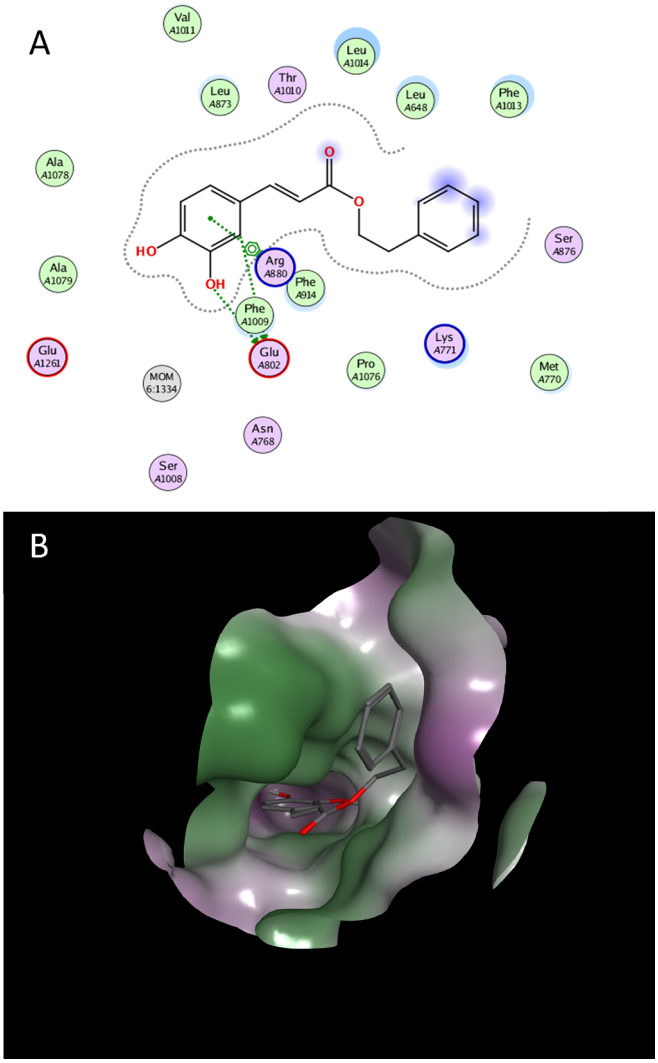

Fig. 6. CAPE interactions with XO. A: 2D ligand/receptor interaction diagram. B: Surface of the binding site coloured according to hydrophobicity, illustrating its amphiphilic character of the site's entrance (purple: hydrophobic, green: hydrophilic).

hydrophilicity profile of the site entrance. This could account for the enhanced activities seen for **8** and **9** with their shorter tethers forcing the B-ring further into the hydrophobic binding site, away from the hydrophilic part of the site entrance and/or solvent molecules. A similar situation was encountered by **7**, which had its hydrophobic bulk located closer towards the core of the pocket than CAPE. Likewise, placing a polar hydroxyl group on the B-ring (**17**, **18**, and **19**) enhanced potency, presumably by allowing these compounds to engage with the polar residues at the site entrance or with solvent molecules. The CAPE analogs in which the phenethyl group was removed or replaced by a short non-polar alkyl residue (**2**, **3**, and **4**) likely experienced an unfavorable loss of hydrophobic interactions but also benefitted from a lack of unfavorable polar/non-polar mismatches at the pocket opening. As a result, no major changes in activity were observed for these compounds.

3.4. Trends in radical scavenging

Among the 20 compounds tested, 16 were capable of scavenging the DPPH radical. Using the stable DPPH radical as a representative species is common practice and provides a good measure for a compound's potential with regard to other, physiologically relevant species, such as the hydroxyl radical or the superoxide anion [42]. As observed previously for coumarins and chalcones [26,27], the distinction between active and inactive compounds was well-defined and depended on the hydroxyl substitution pattern at the two phenyl rings. The inactive compounds **12**, **13**, **14**, and **16** had RSA values close to zero whereas all others displayed clearly noticeable activities (Table 1). Inspection of the structures of the active compounds revealed that they all had hydroxyl groups in 1,2- or 1,4-position at the A-ring. In contrast, the inactive compounds either had only a single hydroxyl group (**12**, **13**, and **14**) or two hydroxyl groups in 1,3-position (**16**). The 1,2- and 1,4-configurations were believed to stabilize the radical generated upon DPPH scavenging via increased resonance [43], which provided a rationale for the observed behavior.

4. Conclusions

We have developed a convenient and effective synthetic route that yields access to a variety of hydroxylated CAPE derivatives. These analogs were the basis for inhibition assays that resulted in the first systematic effort at establishing SARs for XO inhibition by this compound class. We identified **8** as the most promising candidate for further development since it combines the structural requirements for good radical scavenging ability with effective XO inhibition. As we have demonstrated previously, compounds with such a dual property profile can protect cells from oxidative stress [26,27] and therefore hold promise as novel tools to combat reperfusion injuries. The next steps towards achieving this long-term goal involve more comprehensive testing, including assays that evaluate scavenging of radicals of direct physiological relevance, such as the superoxide anion or the hydroxyl radical. Moreover, the postulated potential of compounds such as **8** to protect cells and tissue from oxidatively induced stress will need to be evaluated *in vivo*.

5. Funding sources

This work was supported in part by grants from the National Institutes of Health (Awards 5P20GM103436 and 2R15GM084431-02A1 to S.P.).

References

[1] J. Metzner, H. Bekemeier, M. Paintz, E. Schneidewind, On the antimicrobial activity of propolis and propolis constituents, Pharmazie 34 (2) (1979) 97–102.
[2] D. Grunberger, R. Banerjee, K. Eisinger, E.M. Oltz, L. Efros, M. Caldwell, V. Estevez, K. Nakanishi, Preferential cytotoxicity on tumor cells by caffeic acid phenethyl ester isolated from propolis, Experientia 44 (1988) 230–232.
[3] F. Armutcu, S. Akyol, S. Ustunsoy, F.F. Turan, Therapeutic potential of caffeic acid phenethyl ester and its anti-inflammatory and immunomodulatory effects (Review), Exp. Ther. Med. 9 (5) (2015) 1582–1588.
[4] G. Murtaza, S. Karim, M.R. Akram, S.A. Khan, S. Azhar, A. Mumtaz, M.H. Bin Asad, Caffeic acid phenethyl ester and therapeutic potentials, Biomed. Res. Int. 2014 (2014).
[5] M.F. Tolba, S.S. Azab, A.E. Khalifa, S.Z. Abdel-Rahman, A.B. Abdel-Naim, Caffeic acid phenethyl ester, a promising component of propolis with a plethora of biological activities: a review on its anti-inflammatory, neuroprotective, hepatoprotective, and cardioprotective effects, IUBMB Life 65 (8) (2013) 699–709.
[6] Y. Pommier, A.A. Johnson, C. Marchand, Integrase inhibitors to treat HIV/AIDS, Nat. Rev. Drug Discovery 4 (3) (2005) 236–248.
[7] A. Russo, R. Longo, A. Vanella, Antioxidant activity of propolis: role of caffeic acid phenethyl ester and galangin, Fitoterapia 73 (Suppl 1) (2002) S21–S29.
[8] K. Yoshizumi, N. Nishioka, T. Tsuji, Xanthine oxidase inhibitory activity and hypouricemia effect of propolis in rats, Yakugaku Zasshi 125 (3) (2005) 315–321.
[9] S.H. Wang, C.S. Chen, S.H. Huang, S.H. Yu, Z.Y. Lai, S.T. Huang, C.M. Lin, Hydrophilic ester-bearing chlorogenic acid binds to a novel domain to inhibit xanthine oxidase, Planta Med. 75 (11) (2009) 1237–1240.
[10] F. Borges, E. Fernandes, F. Roleira, Progress towards the discovery of xanthine oxidase inhibitors, Curr. Med. Chem. 9 (2) (2002) 195–217.
[11] P. Pacher, A. Nivorozhkin, C. Szabo, Therapeutic effects of xanthine oxidase inhibitors: renaissance half a century after the discovery of allopurinol, Pharmacol. Rev. 58 (1) (2006) 87–114.
[12] I. Garcia-Valladares, T. Khan, L.R. Espinoza, Efficacy and safety of febuxostat in patients with hyperuricemia and gout, Ther. Adv. Musculoskelet Dis. 3 (5) (2011) 245–253.

[13] K. Nepali, G. Singh, A. Turan, A. Agarwal, S. Sapra, R. Kumar, U.C. Banerjee, P.K. Verma, N.K. Satti, M.K. Gupta, O.P. Suri, K.L. Dhar, A rational approach for the design and synthesis of 1-acetyl-3,5-diaryl-4,5-dihydro(1H)pyrazoles as a new class of potential non-purine xanthine oxidase inhibitors, Bioorg. Med. Chem. 19 (6) (2011) 1950–1958.
[14] K. Nepali, A. Agarwal, S. Sapra, V. Mittal, R. Kumar, U.C. Banerjee, M.K. Gupta, N.K. Satti, O.P. Suri, K.L. Dhar, N-(1,3-Diaryl-3-oxopropyl)amides as a new template for xanthine oxidase inhibitors, Bioorg. Med. Chem. 19 (18) (2011) 5569–5576.
[15] R. Dhiman, S. Sharma, G. Singh, K. Nepali, P.M. Singh Bedi, Design and synthesis of aza-flavones as a new class of xanthine oxidase inhibitors, Arch. Pharm. (Weinheim) 346 (1) (2013) 7–16.
[16] S. Sharma, K. Sharma, R. Ojha, D. Kumar, G. Singh, K. Nepali, P.M. Bedi, Microwave assisted synthesis of naphthopyrans catalysed by silica supported fluoroboric acid as a new class of non purine xanthine oxidase inhibitors, Bioorg. Med. Chem. Lett. 24 (2) (2014) 495–500.
[17] S. Shukla, D. Kumar, R. Ojha, M.K. Gupta, K. Nepali, P.M. Bedi, 4,6-Diaryl/heteroarylpyrimidin-2(1H)-ones as a new class of xanthine oxidase inhibitors, Arch. Pharm. (Weinheim) 347 (7) (2014) 486–495.
[18] C.M. Burns, R.L. Wortmann, Gout therapeutics: new drugs for an old disease, Lancet 377 (9760) (2011) 165–177.
[19] C. Diaz-Torne, N. Perez-Herrero, F. Perez-Ruiz, New medications in development for the treatment of hyperuricemia of gout, Curr. Opin. Rheumatol. 27 (2) (2015) 164–169.
[20] R. Terkeltaub, D.A. Bushinsky, M.A. Becker, Recent developments in our understanding of the renal basis of hyperuricemia and the development of novel antihyperuricemic therapeutics, Arthritis Res. Ther. 8 (Suppl 1) (2006) S4.
[21] D. Dorion, A. Zhong, C. Chiu, C.R. Forrest, B. Boyd, C.Y. Pang, Role of xanthine oxidase in reperfusion injury of ischemic skeletal muscles in the pig and human, J. Appl. Physiol. (1985) 75 (1) (1993) 246–255.
[22] A.A. Khalil, F.A. Aziz, J.C. Hall, Reperfusion injury, Plast. Reconstr. Surg. 117 (3) (2006) 1024–1033.
[23] J.M. McCord, Oxygen-derived free radicals in postischemic tissue injury, New England J. Med. 312 (3) (1985) 159–163.
[24] Y.C. Chang, F.W. Lee, C.S. Chen, S.T. Huang, S.H. Tsai, S.H. Huang, C.M. Lin, Structure-activity relationship of C6–C3 phenylpropanoids on xanthine oxidase-inhibiting and free radical-scavenging activities, Free Radical Biol. Med. 43 (11) (2007) 1541–1551.
[25] H.C. Lin, S.H. Tsai, C.S. Chen, Y.C. Chang, C.M. Lee, Z.Y. Lai, C.M. Lin, Structure-activity relationship of coumarin derivatives on xanthine oxidase-inhibiting and free radical-scavenging activities, Biochem. Pharmacol. 75 (6) (2008) 1416–1425.
[26] E. Hofmann, J. Webster, T. Do, R. Kline, L. Snider, Q. Hauser, G. Higginbottom, A. Campbell, L. Ma, S. Paula, Hydroxylated chalcones with dual properties: Xanthine oxidase inhibitors and radical scavengers, Bioorg. Med. Chem. 24 (4) (2016) 578–587.
[27] E. Hofmann, J. Webster, T. Kidd, R. Kline, M. Jayasinghe, S. Paula, Coumarins with xanthine oxidase inhibiting and radical scavenging properties: Tools to combat oxidativ stress in cells, Int. J. Biosci., Biochem. Bioinform. 4(4) (2014) 5.
[28] M.K. Irmak, E. Fadillioglu, S. Sogut, H. Erdogan, M. Gulec, M. Ozer, M. Yagmurca, M.E. Gozukara, Effects of caffeic acid phenethyl ester and alpha-tocopherol on reperfusion injury in rat brain, Cell Biochem. Funct. 21 (3) (2003) 283–289.
[29] M.K. Ozer, H. Parlakpinar, A. Acet, Reduction of ischemia–reperfusion induced myocardial infarct size in rats by caffeic acid phenethyl ester (CAPE), Clin. Biochem. 37 (8) (2004) 702–705.
[30] B. Ozyurt, M. Iraz, K. Koca, H. Ozyurt, S. Sahin, Protective effects of caffeic acid phenethyl ester on skeletal muscle ischemia-reperfusion injury in rats, Mol. Cell. Biochem. 292 (1–2) (2006) 197–203.
[31] M. Touaibia, M. Guay, Natural Product Total Synthesis in the Organic Laboratory: Total Synthesis of Caffeic Acid Phenethyl Ester (CAPE), a Potent 5-Lipoxygenase Inhibitor from Honeybee Hives, J. Chem. Educ. 88 (2011) 473–475.
[32] S. Son, E.B. Lobkowsky, B.A. Lewis, Caffeic acid phenethyl ester (CAPE): synthesis and X-ray crystallographic analysis, Chem. Pharm. Bull (Tokyo) 49 (2) (2001) 236–238.
[33] H. Shi, D. Xie, R. Yang, Y. Cheng, Synthesis of caffeic acid phenethyl ester derivatives, and their cytoprotective and neuritogenic activities in PC12 cells, J. Agric. Food. Chem. 62 (22) (2014) 5046–5053.
[34] C. Xia, W. Hu, Synthesis of caffeic acid esters, J. Chem. Res. 5 (2005) 332–334.
[35] C.N. Xia, H.B. Li, F. Liu, W.X. Hu, Synthesis of trans-caffeate analogues and their bioactivities against HIV-1 integrase and cancer cell lines, Bioorg. Med. Chem. Lett. 18 (24) (2008) 6553–6557.
[36] Y. Cheng, W.H. Prusoff, Relationship between the inhibition constant (K1) and the concentration of inhibitor which causes 50 per cent inhibition (I50) of an enzymatic reaction, Biochem. Pharmacol. 22 (23) (1973) 3099–3108.
[37] S.D. Sharma, H.K. Rajor, S. Chopra, R.K. Sharma, Studies on structure activity relationship of some dihydroxy-4-methylcoumarin antioxidants based on their interaction with Fe(III) and ADP, Biometals 18 (2) (2005) 143–154.
[38] C.C. Group, Molecular Operating Environment (MOE), 2013.08, Chemical Computing Group, 1010 Sherbooke St. West, Suite #910, Montreal, QC, Canada, 2018.
[39] J.M. Pauff, R. Hille, Inhibition studies of bovine xanthine oxidase by luteolin, silibinin, quercetin, and curcumin, J. Nat. Prod. 72 (4) (2009) 725–731.
[40] C.R. Corbeil, C.I. Williams, P. Labute, Variability in docking success rates due to dataset preparation, J. Comput. Aided Mol. Des. 26 (6) (2012) 775–786.
[41] K. Okamoto, B.T. Eger, T. Nishino, S. Kondo, E.F. Pai, T. Nishino, An extremely potent inhibitor of xanthine oxidoreductase. Crystal structure of the enzyme-inhibitor complex and mechanism of inhibition, J. Biol. Chem. 278 (3) (2003) 1848–1855.
[42] O.P. Sharma, T.K. Bhat, DPPH antioxidant assay revisited, Food Chem. 113 (2009) 1202–1205.
[43] H.M. Ali, A. Abo-Shady, H.A. Sharaf Eldeen, H.A. Soror, W.G. Shousha, O.A. Abdel-Barry, A.M. Saleh, Structural features, kinetics and SAR study of radical scavenging and antioxidant activities of phenolic and anilinic compounds, Chem. Cent. J. 7 (1) (2013) 53.